CIMAC CONGRESS 23
BUSAN, JUNE 12 –16, 2023

2023 | 651

Optimization of Complex Energy Systems as an Enabler for Sustainable Shipping Solutions

System Integration & Hybridization

Bernhard Thaler, Large Engines Competence Center Graz

Michael Wohlthan, Large Engines Competence Center Graz
Gerhard Pirker, Large Engines Competence Center Graz
Christof Gumhold, Large Engines Competence Center Graz
Christoph Redtenbacher, Large Engines Competence Center Graz
Andreas Wimmer, Graz, University of Technology

ABSTRACT

Energy systems both in offshore and onshore applications continue to increase in complexity. The drive for sustainable solutions calls for the integration of new technology solutions that couple all available energy forms such as electricity, heat and fuels. For ships, the traditional energy system with main and auxiliary engines is complemented by hybrid solutions, energy storages, fuel flexibility including renewable fuels, exhaust aftertreatment including carbon capture, and thermal energy recovery. The design and optimization of such complex systems can only be achieved with highly flexible simulation models that are capable of covering technical aspects (e.g. system layout, selection of components, component specifications and operating strategy), environmental aspects (e.g., greenhouse gas emissions) and economical aspects (e.g., CAPEX).

This paper presents a holistic approach for simulating and optimizing energy systems as well as comparing various component technologies within the system. Using a modular approach, it connects various energy components via energy and mass flows. Each component can be modeled at any level of detail, from preset maps up to detailed physical or data-driven models, for which the methodology provides the necessary system framework and data interface. The system layout as well as the operating strategy can be either specified individually or optimized via mathematical optimization techniques with respect to custom techno-economic or ecologic target functions.

An overview of the versatility of the modular approach is provided for various examples of ship energy systems. Different propulsion energy systems are compared based on their techno-economic performance as well as greenhouse gas emissions, including conventional fossil fuel-based drives, carbon capture systems, hybrid approaches with batteries and complete carbon-neutral powertrains. The results give insight into the optimal layout and operating strategy for the shipping energy concepts of the future, providing information for all stakeholders in the maritime transport sector, from engine suppliers to ship operators and policy regulators.

1 INTRODUCTION

Sustainable energy systems based on renewable energy are continuing to supply ever greater shares of the global energy mix. This trend is driven by decreasing costs of emerging technologies, energy security concerns, and climate policy [1]. The maritime industry, which is responsible for 3% of global CO_2-emissions [2], is making efforts to phase out fossil fuel-powered systems through both technological and regulatory means. Starting in 2024, the European Union will be incorporating all ship emissions within its territory and half of the emissions of incoming and outgoing ships into its Emission Trading System (ETS) [3]. The International Maritime Organization (IMO) is planning to update its Greenhouse Gas (GHG) reduction strategy in 2023 and strengthen its ambition towards a complete climate neutral fleet until 2050 [4].

For sustainable applications, the goal of energy systems operation is to cost-effectively integrate renewable energies by selecting the appropriate technologies, designing an optimal system, and utilizing smart control strategies for efficient utilization of all energy resources. Optimizing the future energy system of a ship presents the same challenges as onshore power systems. In addition to the importance of energy-saving measures such as improved hydrodynamic designs, the complete elimination of the ship's CO_2 emissions necessitates more advanced concepts. Depending on the application, promising strategies may include direct electrification using battery energy storage [5], renewable fuels [6], hybrid solutions [7], or carbon capture to prevent the emission of CO_2 into the atmosphere [8].

In order to identify the most effective layout of such systems, highly flexible simulation tools must be employed to compare different technology options for varying use cases and to select the best configurations for optimal performance. This paper introduces an adaptable approach based upon an energy flow-based optimization framework for generic energy systems (LEC ENERsim). The technique involves connecting various system components that can be modeled with tailored technological detail. Component classes include, for instance, energy consumers, storage units, energy sources, or converters. The approach takes into account technological, economic, and operational limitations on system operation. It can be utilized for all applications of both onshore and offshore setups which involve a complex interplay of different energy forms such as electricity, heat, fuels, or mechanical energy. Consequently, a full sector coupling of such hybrid systems is fully encompassed in the framework's architecture.

In this paper, various energy system configurations are compared for two distinct ship use cases. The first vessel is a container ship operating on a multi-day route between East Asia and Europe; the second is a Ro-Pax ferry traversing the Baltic Sea with a typical daily voyage. For each, different propulsion setups are evaluated, including a traditional fossil-fuel based powertrain, a hybrid solution incorporating renewable fuels, a battery powertrain, and a system that incorporates onboard carbon capture. The optimal design of each system is determined and the results are compared according to techno-economic and environmental criteria.

2 SYSTEM SIMULATION BASED ON ENERGY FLOW OPTIMIZATION

The framework allows to model energy systems based on generic energy flows between the system components. Energy flows are considered for all time steps of the desired simulation time span, with custom time resolution. The system model is formulated in the mixed-integer linear programming framework, with characteristic constraints for different component models that are grouped in specific module types. Example systems that can be modelled are shown in Figure 1, and include ship energy systems, microgrids, hybrid power plants, and macro-energy systems. The code is formulated in python, and a graphical user interface exists to set up the system in LEC ENERsim, parametrize components, and analyze results. In the following, the basic concepts of the methodology as well as the required system components are briefly presented. For more details on specific model implementations recently published literature is referred to [9] [10].

2.1 Target functions

The methodology optimizes energy flows $E_{c,c,'t}$ between components c and c' at all timesteps t of a required time span, considering various operational boundaries. Optimization is performed with respect to a specific target function. Possible target functions are, for example:

- **Economic costs:** The sum of all investment costs for all components, fuel costs, fixed and variable operating costs, costs for energy purchased from grids, and incomes from energy sold to grids.
- **CO_2 emissions:** Includes all emissions related to fossil fuels used within the systems, and emissions related to energy purchased from grids (e.g., grid electricity is considered with its specified CO_2-intensity).

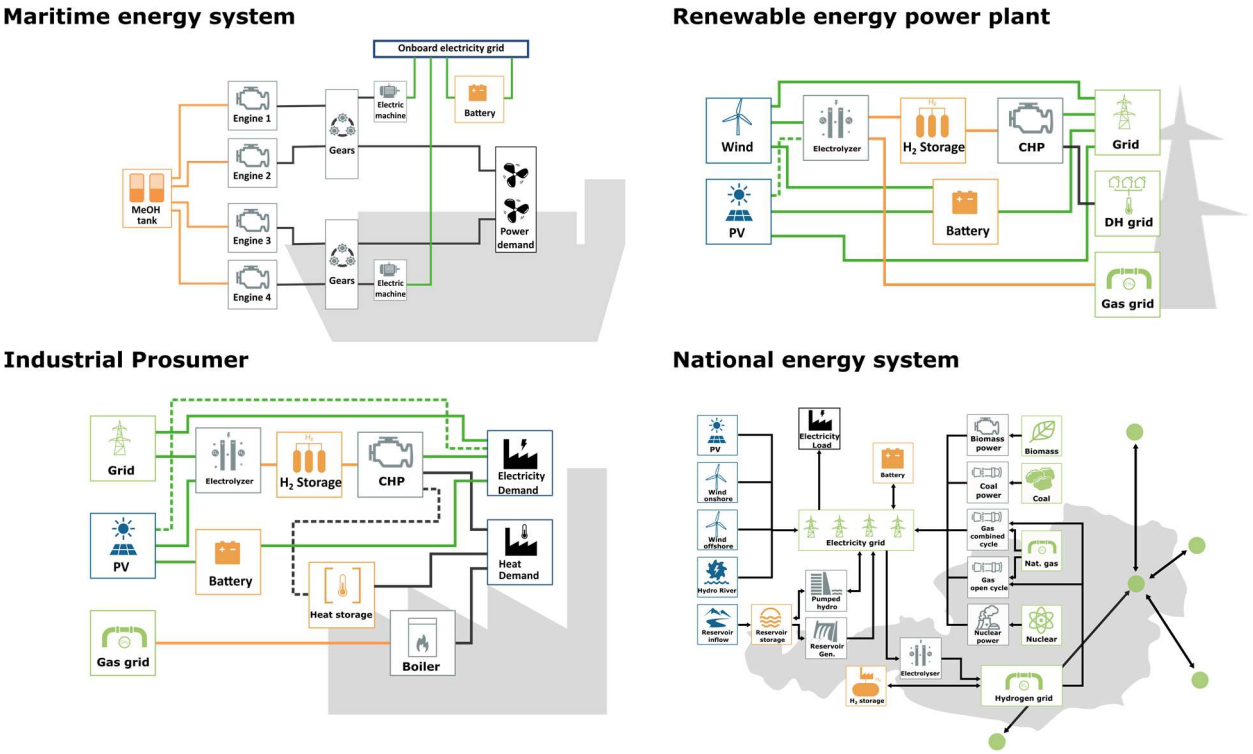

Figure 1: Examples of energy systems realized with the LEC ENERsim framework. Systems consist of specific component classes: sources (blue), converters (grey), storage units (orange), grids (green) and demands (black).

- **Energy efficiency:** Defined as ratio of output energy to input energy.
- **Degree of autarchy:** Defined as ratio of self-generated energy (e.g., local renewable energy) to total energy used.

Combinations of target functions in a multi-objective optimization are also possible, leading to Pareto-optimal solution manifolds. For example, an optimization could aim at a reduction in CO_2 emissions while achieving minimal economic costs. Output of the optimization are operational trajectories that fulfill the constraints described in the following sections. In addition, all relevant components can be optimized in their sizes to fulfill all required boundaries while minimizing the target function. Systems are set up using components of specific classes, which are shortly summarized in the following.

2.2 Energy demand

Energy demands constitute energy sinks, with a specific load profile $E_{d,t}$, that has to be fulfilled by energy flows $E_{c,d,t}$ from neighboring components c at all time steps t:

$$\sum_c E_{c,d,t} = E_{d,t}\ , \forall t \qquad (1)$$

Examples include a ship propulsion demand profile, electricity load profiles, or thermal energy loads.

2.3 Energy source

Energy sources are characterized by an energy profile $E_{s,t}$ of which the energy has to be distributed via energy flows $E_{s,c,t}$ to connected components c for all time steps t:

$$E_{s,t} = \sum_c E_{s,c,t}\ \ , \forall t \qquad (2)$$

Examples include renewable energy sources such as photovoltaics or wind power plants.

2.4 Energy grid

Energy grids can act as either sinks or sources of energy, where energy can be bought ($E_{g,c,t}$) or sold ($E_{c,g,t}$), respectively, up to a specified installed grid power P_g^{max}:

$$\sum_c E_{c,g,t} + \sum_c E_{g,c,t} \leq P_{g,max} \cdot \Delta t, \quad \forall t \qquad (3)$$

Note that the time resolution Δt is introduced for the conversion between energy and power. Examples include electricity grids, heat grids, or gas grids. Grids are also characterized by economic market data, with fixed or time dependent energy prices.

2.5 Energy storage

Storage units are characterized by their energy capacity CP_s and maximum charge/discharge power P_{max}^s:

$$C_{s,t} \leq \mathrm{CP_s},\ \forall t \quad (5)$$

$$\sum_c E^{in}_{c,s,t} \leq P^s_{\max} \cdot \Delta t\ ,\forall t \quad (6)$$

$$\sum_c E^{out}_{s,c,t} \leq P^s_{\max} \cdot \Delta t\ ,\forall t \quad (7)$$

The energy content (charge) $C_{s,t}$ at all time steps is based on the balance of energy inflows ($E^{in}_{c,s,t}$) and outflows ($E^{out}_{s,c,t}$) from components c, which are corrected by the roundtrip efficiency $\eta_{s,roundtrip}$ of the storage unit:

$$C_{s,t} = \mathrm{C_{s,(t-1)}} + \sum_c E^{in}_{c,s,t} \cdot \sqrt{\eta_{s,roundtrip}} - \sum_c \frac{E^{out}_{s,c,t}}{\sqrt{\eta_{s,roundtrip}}}\ ,\forall t \quad (8)$$

Examples for storage units are fuel tanks, battery cells, or hot water thermal storage tanks.

2.6 Energy converter

Converters transform or distribute energy flows of connected components. The energy form can thereby change (e.g., from chemical to electric energy) with the result of energy loss according to the converter's efficiency. Main parameters of converters are their nominal power P^c_{max}, and their efficiencies η_c, where the latter can be specified either through constant values or characteristic curves.

$$\sum_{c'} E^{in}_{c',c,t} \leq P^c_{\max} \cdot \Delta t\ ,\forall t \quad (9)$$

$$\sum_{c'} E^{in}_{c',c,t} \cdot \eta_c = \sum_{c'} E^{out}_{c,c',t}\ ,\forall t \quad (10)$$

The efficiency defines the losses that occur while transforming input energy flows $E^{in}_{c,c',t}$ to output energy flows $E^{out}_{c,c',t}$, where c is the converter and c' is a neighboring component. Examples for converters are engines, electrolyzers, heat pumps, boilers, or fuel cells.

3 CASE STUDY: ANALYSES OF SHIP SYSTEMS

This paper compares the performance of several ship energy system configurations for two distinct vessel types: a container ship operating on transoceanic long-distance routes and a Ro-Pax ferry operating on a smaller, fixed daily route. For both vessels, several identical energy system configurations, shown in Figure 2, were set up and compared. The investigated configurations include:

1. A conventional fossil fuel-based powertrain using heavy fuel oil (HFO, low sulfur) for propulsion engines, auxiliary gensets, and boilers.
2. A hybrid configuration with the addition of a battery. Engines and boilers use renewable methanol (Re-MeOH) as fuel.
3. A battery electric powertrain using no liquid fuel for propulsion and on-board electricity. HFO is still used for thermal energy generation in the boiler.
4. A hybrid configuration using HFO for the propulsion engine and the boiler, and liquid hydrogen (LH_2) converted in fuel cells for the auxiliary electricity demands.
5. A system running on HFO and an onboard carbon capture unit based on chemical absorption to capture CO_2 emissions. Energy flows for onboard CO_2-handling (compression, liquefaction) are also considered.

Except for the battery-electric powertrain, all configurations use one large 2-stroke main engine for direct propulsion. Hybrid setups use a shaft generator connected to this engine to convert mechanical energy to electric energy and vice versa. The propulsion engine is equipped with an exhaust waste heat boiler that can supply onboard thermal energy demands. Except for the battery-electric system, all setups use auxiliary engines or fuel cells for onboard electricity generation, and a fuel-powered boiler for heat generation. All system configurations are simulated both for the container ship and the Ro-Pax ferry. The difference between the two vessels lies in their load profiles of propulsion, electricity and heat (Figure 3). Heat loads consist of, for example, fuel heating, galley heating, or space and water heating. The ferry heat load is, in relative terms to the propulsion load, larger than the one of the container ship since it has a higher space heating demand. The energy loads have to be delivered by the energy system at all time steps of the simulation. As can be seen in Figure 3, the load of the container ship stretches over approximately 80 days, representing one roundtrip between Europe and East Asia with multiple intermediate stops. The load profile of the ferry covers 17 hours, representing a one-way trip within the Baltic Sea. System parameters and overall economic assumptions are summarized in Table 1. The economic model assumes a new-build of all configurations. For fuel costs, central estimates for near-term production costs of Re-MeOH and LH_2 from the Bureau Veritas white paper on alternative fuels outlook for shipping are used [11]. Techno economic parameters of the components are listed in Table 2. For the investment costs, only technologies that are relevant for the propulsion system are considered. Remaining other costs of the ship such as hull, onboard equipment for accommodation and freight

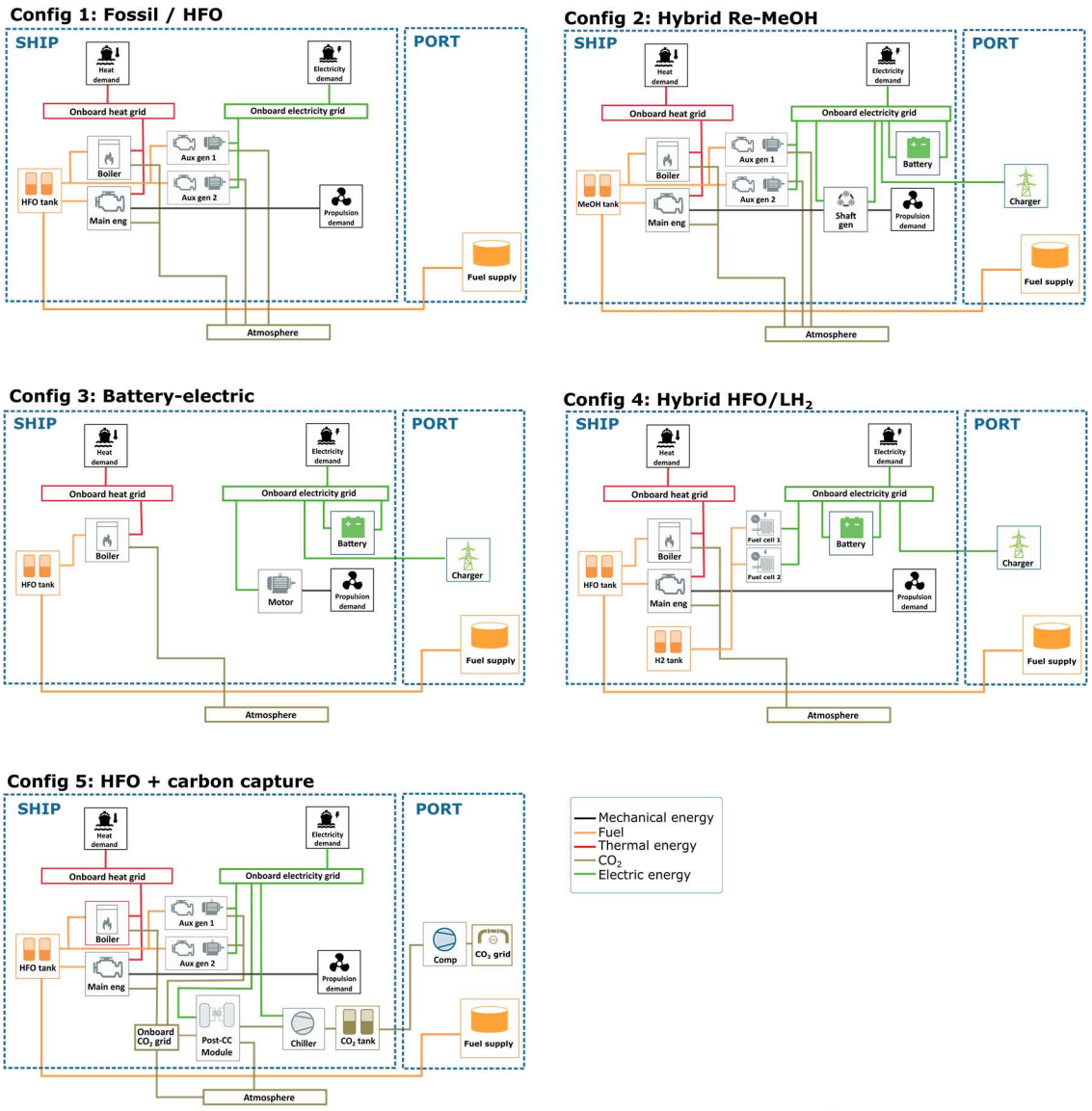

Figure 2: Investigated ship energy system configurations. All systems consist of an energy system that supplies the mechanical propulsion load, onboard heat and onboard electricity loads.

management are assumed to be the same for all configurations and are excluded, as they would only add an offset to cost comparisons. Engine efficiencies are modelled based on representative, load- dependent curves retrieved from public manufacturer data using data on fuel consumption, exhaust mass flows, and exhaust temperatures. The same engine efficiency is assumed for HFO- and Re-MeOH engines, Thermal efficiencies of exhaust gas- and fuel boilers are calculated based on exhaust enthalpies and the required steam temperature level of the heat demand. All converter units except engines are modelled using load-independent efficiencies. Fuel cells are assumed to be of the type Proton-exchange membrane (PEM). The storage units (battery, fuel tanks, LH_2) are allowed to be charged during port stays, the respective time windows are indicated in Figure 3 as those times where the propulsive loads are zero. The carbon capture system uses chemical absorption with an amine-based solvent. Energy demands of the carbon capture system constitute thermal energy in the form of saturated steam to regenerate the amine solvent, and electrical energy for auxiliary pumps. CO_2 storage discharge of the carbon capture system is assumed to be possible during all port stays. CO_2 is stored in tanks in a liquefied and pressurized state at a temperature of -15 °C and 20 bar. All storage unit charges are constrained to reach the same charge at the end of the simulation time span in order to correctly account for fuel consumption at the end of the simulation. When a battery is part of the system, it is allowed to be charged during all port stays. The battery of the hybrid configurations (C2 and C4) can be used both as energy storage and for balancing the engine load curve, enabling more

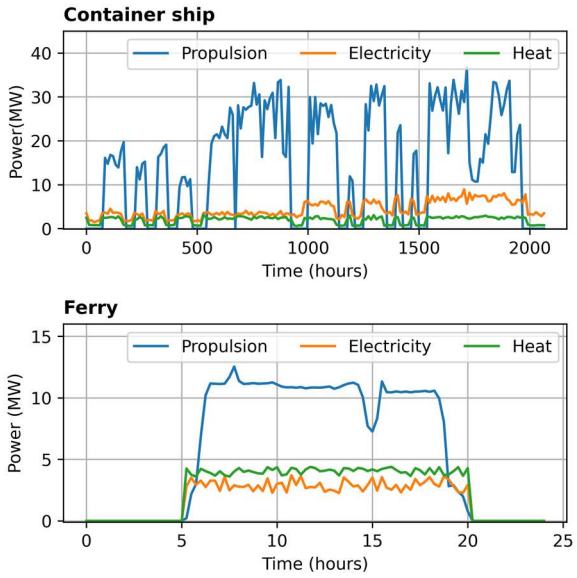

Figure 3: Load profiles for propulsion, electricity and heat for the two investigated applications.

smooth operation with higher efficiency. The systems that have a charging connection for the battery are also allowed to use the port charging infrastructure to supply the onboard electricity demand while the ship is anchored. Port electricity, Re-MeOH and H_2 are assumed to be CO_2 neutral and have zero emission intensity. LH_2 boil off is not explicitly modelled, the emerging fuel is thought to be directly used for power generation.

The configurations are set up in the ENERsim framework and the system design and operation are optimized. As a result, optimal component sizes and optimal energy management strategies are retrieved. The results are compared based on several techno-economic performance indicators, which are:

Table 1: Basic system and economic data.

Parameter	Value	
Overall ship		
Lifetime	30	Years
Container ship type	10 000	TEU
Ferry	11 000	dwt
Steam grid temperature (hotel load)	130	°C
Steam grid temperature (carbon capture)	150	°C
Basic economic data		
Assumed base year	2030	near-term scenario
HFO price	48	€/MWh
Port (renewable) electricity price	60	€/MWh
LH_2 price	112	€/MWh
Re-MeOH price	210	€/MWh

- Annualized costs (C_a), which are calculated with:

$$C_a = \sum_c [(I_c + R_c - S_c) \cdot crf + O_c^{fix}] \cdot P_c + \sum_{cc't} O_c^{var} \cdot E_{c,c',t} + \sum_{Fuel-grid,c,t} E_{Fuel-grid,c,t} \cdot f_c \quad (11)$$

where I_c, R_c and S_c are the investment costs, re-investment costs and end-of-life salvation incomes for each component c, respectively. *crf* is the capital return factor, which accounts for interest rate and inflation, O_c^{fix} are fixed operating costs, P_c is the power of the respective component, O_c^{var} are variable operating costs and f_c is the fuel cost, which is multiplied by the actual bunkered energy flow (electricity, fuel). Both the operating costs as well as the fuel costs are multiplied by an

Table 2: Techno-economic parameters of components used.

Component	Efficiency / Energy demand		CAPEX		OPEX	Lifetime	Source
Propulsion engine	Mechanic	46 %	240	€/kW	2%	25	[12]
	Thermal	15 %					
Auxiliary genset	Mechanic	36 %	240	€/kW	2%	25	[12]
Electric machine		97 %	85	€/kW	2%	25	Assumption
Shaft generator		97 %	85	€/kW	2%	30	Assumption
Gas / fuel boiler		93 %	70	€/kW	2%	25	[13]
Fuel cell		55 %	1100	€/kW	2%	8	[14]
Carbon capture unit	Capture efficiency	85 %	480	€/kg_{CO2}/h	5%	25	[15]
	Thermal energy	4 GJ_{therm}/t_{CO2}					
	Electric energy	0.02 GJ_{elec}/t_{CO2}					
Battery	Roundtrip	90 %	236	€ / kWh	2.5%	15	[16]
MeOH/HFO storage	Roundtrip	100 %	0.1	€/kWh	2%	25	[17]
LH_2 storage	Roundtrip	100 %	1.71	€/kWh	2%	25	[14]
CO_2 storage	Storage conditions	15 bar, -30°C	3	€/kg	5%	25	[18]
CO_2 liquefaction	Energy demand	0.26 GJ_{elec}/t_{CO2}	700	€/kg_{CO2}/h	5%	25	[18]

extension factor to yield yearly values and correctly account them with regard to the annualized investment costs.

- Annual CO_2 emissions (E_{CO_2}) are calculated with:

$$E_{CO_2} = \sum_{fuel-grid,c,t} E_{fuel-grid,c,t} \cdot e_f, \quad (12)$$

as multiplication of the energy flows with the fuel's CO_2 emission intensity e_f. For configuration 5, the captured CO_2 is subtracted from this value.

- Overall energy efficiency E_{eff}, defined as:

$$E_{eff} = \sum_{demands,t} D_{c,t} \; / \; (\sum_{storages} [C_{storage,t_0} - C_{storage,t_{end}}] + \sum_t E_{Port\ electricity,t}), \quad (13)$$

which is the sum of all energy demands divided by the actual energy used.

- Space requirements of the fuel tanks, calculated by multiplication of all relevant storage capacities with the volumetric energy density of the respective fuel.

4 RESULTS

The applied energy systems for the two use cases are compared based on their optimized system designs, operation, and various techno-economic performance indicators. Table 3 gives an overview of the optimized sizes of the system components for all configurations. It can be seen that no battery is installed for the hybrid container ship configuration (C2 and C4), whereas one is installed for the ferry ship configurations. Figure 4 shows Sankey diagrams for selected energy system configurations: the Re-MeOH hybrid configuration (Figure 4a) and the fuel cell hybrid configuration (Figure 4b) for the ferry and the carbon capture configuration (Figure 4c) for the container ship. In the Re-MeOH configuration, no CO_2 emissions that are transferred to the atmosphere are balanced because methanol is thought to be synthesized entirely on direct air captured carbon. In the fuel cell hybrid ferry configuration (Figure 4b), parts of the thermal energy demand can be fulfilled by the exhaust heat recovery, for the rest, the boiler is used. The battery is used sparingly since its size is rather small. Port electricity is supplied both directly to the system, and is used to charge the battery while at anchor. The carbon capture application (Figure 4c) uses much larger boilers and more thermal energy compared to the other two examples, owing to the large thermal demand of the carbon capture module. As can be seen, the energy demand for CO_2 liquefaction is small

Table 3: Optimized component sizes for the 5 configuration cases for both vessels

Component	C1: Baseline	C2: Re-MeOH Hybrid	C3: Battery-electric	C4: HFO/LH2	C5: Carbon capture
Propulsion engine					
Container ship	37.1 MW	47.0 MW	-	37.1 MW	40.3 MW
Ferry	13.0 MW	16.0 MW	-	13.0 MW	13.6 MW
Aux. gensets / Fuel cells					
Container ship	4.2 MW	0.0 MW	-	7.7 MW	5.3 MW
Ferry	1.8 MW	0.0 MW	-	2.0 MW	2.3 MW
Boiler					
Container ship	3.3 MW_{therm}	2.9 MW_{therm}	3.2 MW_{therm}	3.1 MW_{therm}	34.9 MW_{therm}
Ferry	4.4 MW_{therm}	3.2 MW_{therm}	4.5 MW_{therm}	4.4 MW_{therm}	17.3 MW_{therm}
Fuel tank					
Container ship	30621 MWh	29384 MWh	1128 MWh	22099 MWh	44437 MWh
Ferry	463 MWh	384 MWh	63 MWh	340 MWh	679 MWh
Battery					
Container ship	0.0 MWh	0.0 MWh	14989.5 MWh	0.0 MWh	0.0 MWh
Ferry	0.0 MWh	10.0 MWh	204.6 MWh	10.0 MWh	0.00MWh
CO_2 capture system					
Container ship	-	-	-	-	37.0 $t_{CO2/h}$
Ferry	-	-	-	-	14.9 $t_{CO2/h}$
Port charger					
Container ship	-	7.6 MW	72.6 MW	7.6 MW	-
Ferry	-	2.0 MW	41.1 MW	2.0 MW	-

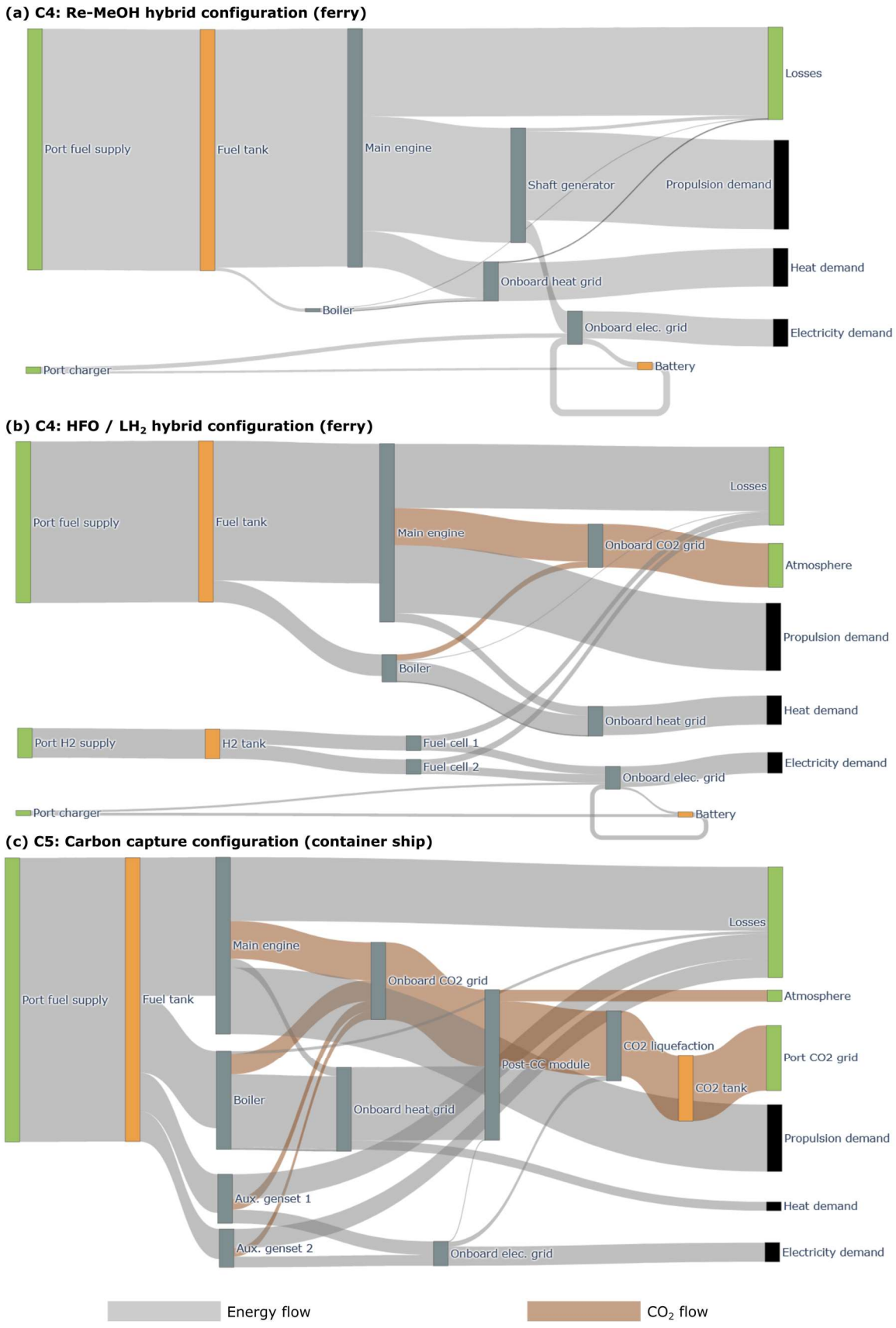

Figure 4: Sankey diagrams of representative configurations. The colors of the components represent their respective classes, which are energy grids (green), converters (grey), storage units (orange) and demands (black). Panel (a) shows the energy flows of the Re-MeOH hybrids configuration of the ferry ship application. Panel (b) shows the energy and CO_2 flows of the fuel cell hybrid configuration of the ferry ship application. Panel (c) shows all flows of the carbon capture configuration of the container ship application.

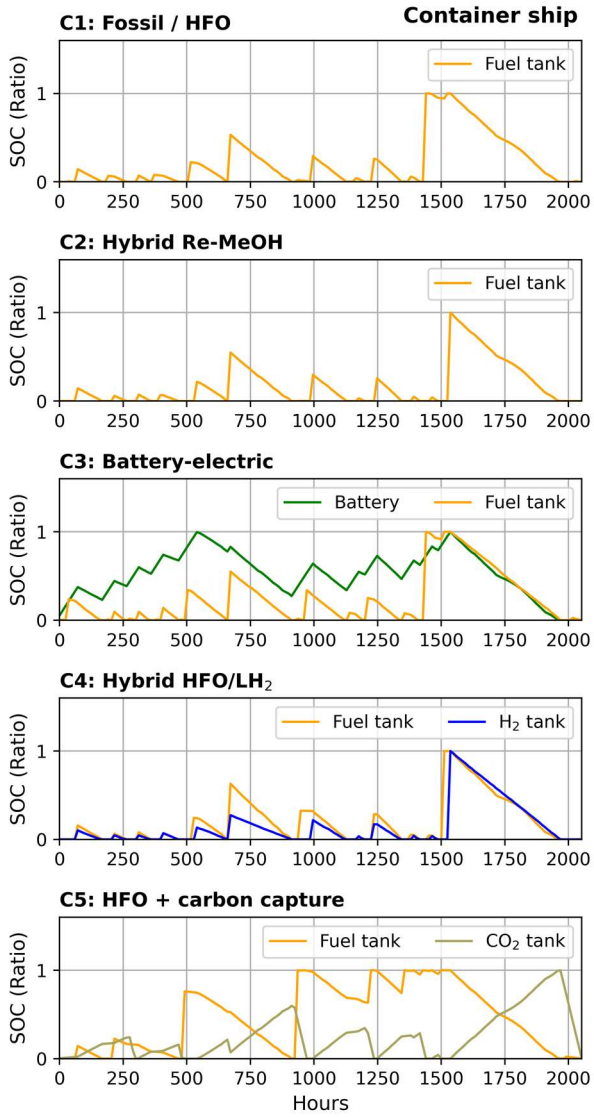

Figure 5: Transient storage charge levels, as result of the container ship operational optimization.

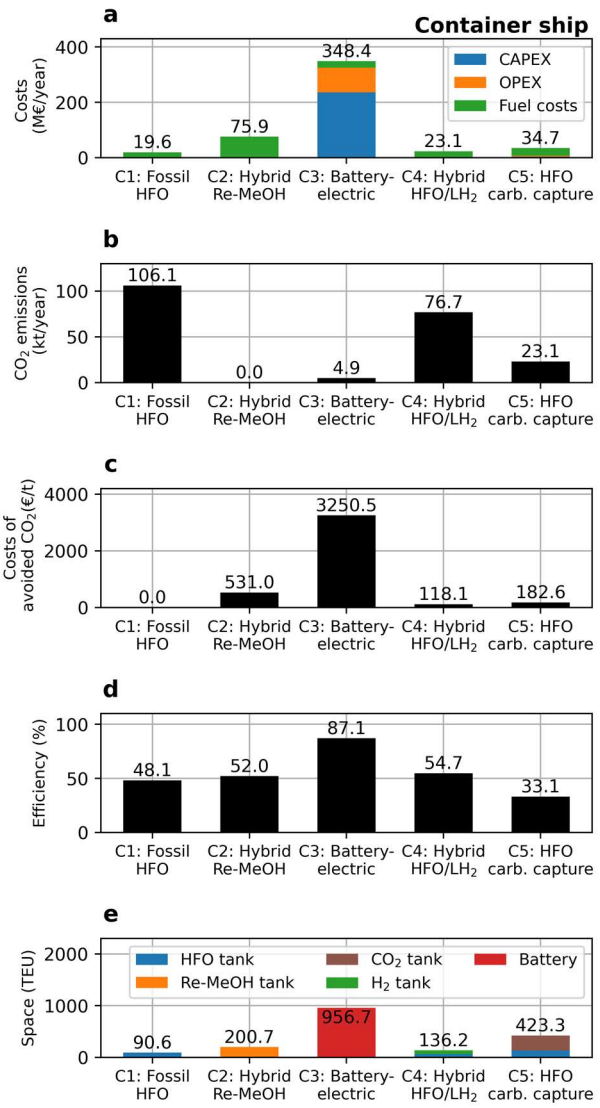

Figure 6: Techno-economic performance indicators of the different configurations for the container ship application. Panel (a) shows the annualized economic costs, panel (b) the annualized CO_2-emissions, panel (c) the CO_2 abatement costs, panel (d) the overall system efficiency, and panel (e) the space requirement of the storage units (tanks and battery) in terms of Twenty-foot Equivalent Units (TEU).

compared to the overall energy demand of the ship. Overall losses of the auxiliary gensets are higher than the losses of the main engine because of the lower efficiency and no installed exhaust gas heat recovery system.

4.1 Container ship

Figure 5 shows the container ship's transient storage charge levels as result of the operational optimization of the different configurations. The charge levels are normalized and indicate the times at which the respective storage units are charged (ports) and discharged (sea). As outlined in the previous section, storage units are allowed to be charged, and in the case of the CO_2 tank also discharged in all ports along the voyage. The same fuel and electricity prices are assumed at all ports. These assumptions have direct consequences on the optimized size of the storage units' maximal capacities, because the optimizer minimizes their sizes so that the demand profiles can be just fulfilled. In the case that charge/discharge would not be possible at all port stays, or fuel prices in the ports would diverge, other operational profiles might result. Figure 6 shows techno-economic performance indicators of the container ship. The major costs of all configurations except the battery-electric powertrain are fuel costs (Figure 6a). For the chosen boundaries, the cheapest configuration is the fossil baseline case, which however also has the highest CO_2 emissions (Figure 6b). Note that no CO_2 costs are included in the cost calculation. However, for all configurations costs of avoided

CO_2 can be calculated (Figure 6c), which is based on the difference in CO_2 emissions and cost compared to the baseline case. These costs can be seen as a fictional CO_2 price that would be needed in order to make the respective system competitive to the baseline case. The highest absolute costs and also avoided CO_2 costs are retrieved for the battery-electric configuration, where the high capital expenditures of the battery dominate. However, since renewable electricity is assumed, fossil emissions are nearly zero and stem only from heat generation by the fossil-fueled boiler. The battery electric-system is also the system with the highest efficiency (Figure 6d). However, the battery also uses the most space because of its low volumetric energy density (Figure 6e). Adding a cost term to the volume ("cost of lost cargo") would make the battery configuration even more expensive. As outlined above, the battery is assumed to be chargeable in all ports. With the installed battery size of 15 GWh and the assumed operational profile, a port charger connection of 73 MW would be necessary (Table 3). A non-available port charging connection at any port location would increase both the required battery size and the charging power in order to deliver sufficient energy during port stays. The second most expensive configuration is the Re-MeOH hybrid system, which is mainly driven by high fuel costs. This system is however the only system that is able to completely eliminate CO_2 emissions, as no fossil fuels are used. The system efficiency of the Re-MeOH system is higher than that of the fossil case owing to the hybrid setup. Also without an installed battery, shore power already reduces fuel consumption, and the installed shaft generator enables an efficient use of the main engine to also supply onboard electricity demands. The space requirements of the Re-MeOH tank is roughly twice as large as the HFO tank, owing to the lower volumetric energy density of methanol. Configuration 4 with the LH_2 driven fuel cells for onboard electricity production results in only a slight cost increase compared to the fossil baseline case and has the lowest costs of avoided CO_2. Owing to the high efficiency of the fuel cell, the overall system efficiency is the second highest after the battery-electric powertrain. In terms of space requirement, the low volumetric density of liquid hydrogen causes however a large space requirement. It is noted that the fuel cell configuration still uses a fossil-fuel powered main engine to deliver the propulsion load, and the overall impact of only changing the gensets is therefore limited. The carbon capture configuration requires the second lowest avoided costs of all decarbonisation options. The assumed maximal capture rate lies at 85%, which is reached during normal operation. However, the actual CO_2-reduction compared to the fossil baseline case is lower, since the energy demand of carbon capture increases fuel consumption. The carbon capture configuration has the lowest energy efficiency (Figure 6d). The additional energy needed consists mostly of thermal energy from the boiler, which is used to deliver heat to the capture unit's reboiler for solvent regeneration. The avoided emissions of CO_2 are approximately 80% of the baseline emissions. With regards to onboard space requirements (Figure 6e), especially the CO_2-tanks require significant additional volume, in addition to larger fuel tanks due to the higher fuel consumption.

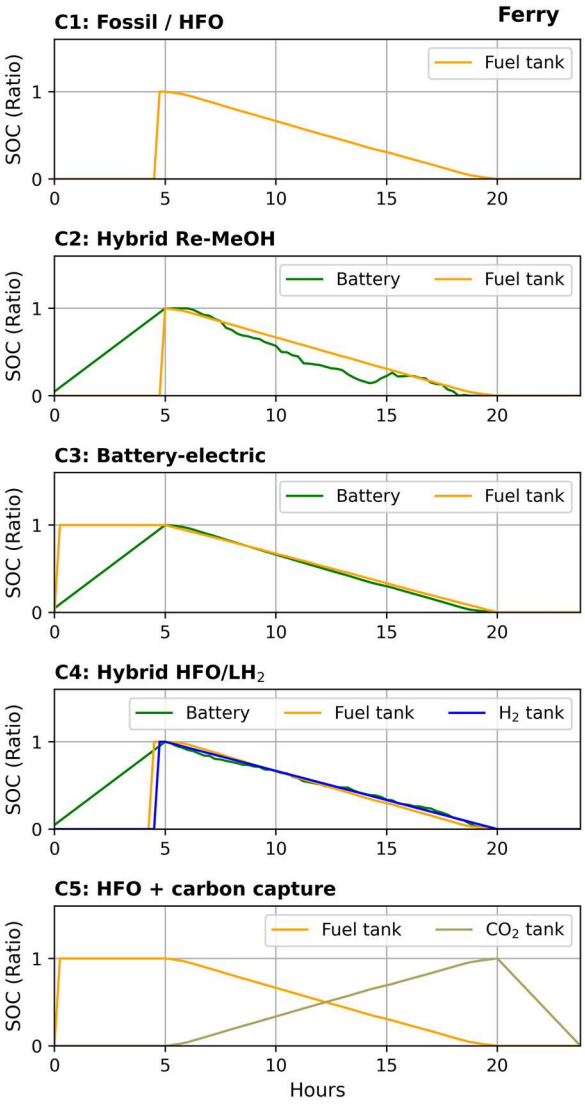

Figure 7: Transient storage charge levels, as result of the ferry ship operational optimization.

4.2 Ferry

Figure 7 shows the transient storage charge levels of the different configurations for the ferry use case. As also already illustrated in Figure 3, the simulated

operating profile of the ferry fundamentally differs from that of the container ship. Only one roundtrip is simulated, which influences the storage charge trajectories. The fuel tanks exhibit only one charge-discharge cycle and the route contains no intermediate port stays. For the hybrid configurations (C2 and C4), the optimized systems use a battery as buffer for a more efficient engine and fuel cell operation. Figure 8 shows the techno-economic performance indicators of the ferry. As for the container ship a strong contribution of fuel costs can be observed (Figure 8a). As strongest contrast to the containership, the battery-electric configuration exhibits much lower costs, and even becomes cheaper than the option with Re-MeOH. The required battery size is smaller for the ferry ship and more full charge cycles are achieved over the year. The fixed daily operation improves the economics of the capital-intensive battery investment. In terms of space requirements (Figure 8e) the battery still uses much more volume compared to the other configurations. The Re-MeOH hybrid configuration is the most expensive option for the ferry application. It shows approximately four times higher costs compared to the HFO baseline. Comparison between all efficiencies of container ship (Figure 6d) and ferry (Figure 8d) reveals higher efficiencies for the ferry for all configurations. The reason for this difference lies in the higher onboard heat loads of the ferry, which lead to a better exploitation of fuel energy because more exhaust heat energy can be used. The carbon capture option is again the least efficient option also for the ferry application. The efficiency drop compared to the other configurations is even more pronounced. Because of the higher onboard heat demand the exhaust gas energy is not available for solvent regeneration and must therefore be substituted by the fuel boiler. The lower efficiency also leads to a larger space requirement because more fuel and CO_2 must be stored on board.

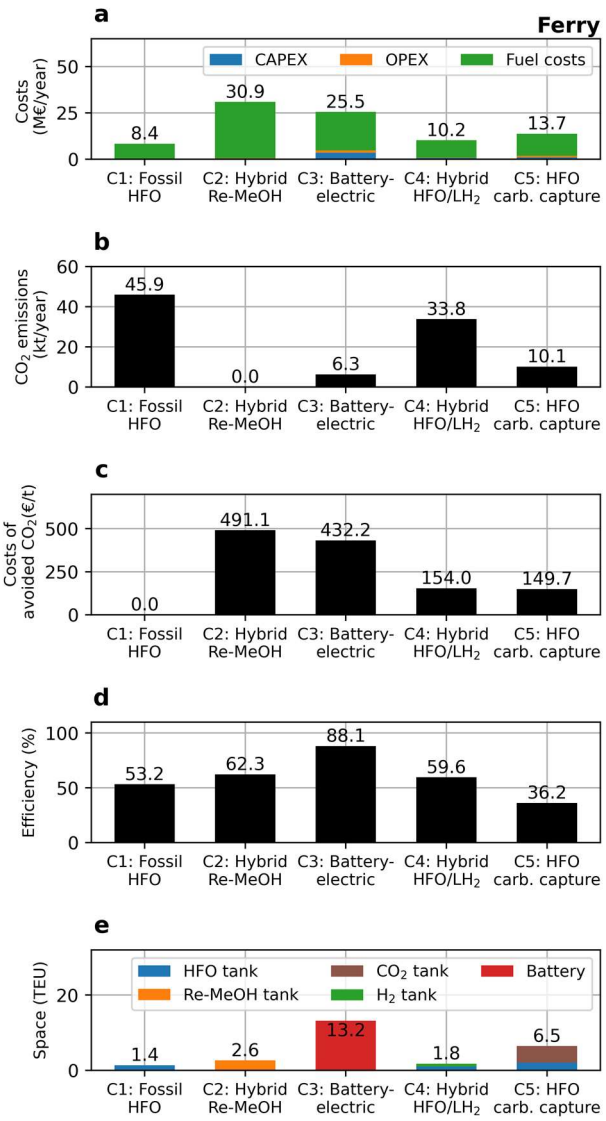

Figure 8: Techno-economic performance indicators of the different configurations for the ferry ship application. Panel (a) shows the annualized economic costs, panel (b) the annualized CO_2-emissions, panel (c) the CO_2 abatement costs, panel (d) the overall system efficiency, and panel (e) the space requirement of the storage units (tanks and battery) in terms of Twenty-foot Equivalent Units (TEU).

5 CONCLUSIONS

The results of this study demonstrate that energy system optimization for ships can provide insights into the potentials and performance of different pathways for sustainable shipping. The generic representation of the technologies allows for comparison on a techno-economic basis. In this paper, the simulation platform LEC ENERsim was used to explore two representative vessel use cases in order to identify optimal arrangements and operation strategies. The chosen method designs all system components to meet the representative energy demand profiles. In reality, fuel tanks or engines may be oversized as a safety margin. The economic and environmental performance of certain technology options are heavily influenced by the choice of techno-economic input parameters such as efficiencies and investment costs. In the cases investigated, for example, battery-electric propulsion exhibited rather high costs; however, this may change with a decrease in battery module prices and electricity prices. Additionally, future fuel costs are highly uncertain, and results must be checked for different scenarios. Furthermore, systems are always subject to certain temporal and spatial limits that are not considered or modelled as fixed boundaries. As an example, the primary energy input (fuel, electricity) was assumed with fixed prices and to be infinitely available; both of these assumptions may not hold true, particularly in an

accelerating energy transition. Similarly, it was assumed that the captured CO_2 discharged from the ship is directly fed into a pipeline with an unknown destination, with no costs for final storage or re-use. Despite these uncertainties, the method can be easily extended with sensitivity studies that could reveal which cost scenarios would make certain technology options viable. The paper only discussed a subset of the multitude of possible solutions for sustainable ship systems. Future focus might also be placed on systems using other fuels such as biofuels, ammonia, synthetic hydrocarbons, new heat technologies such as heat pumps or heat storage, new converters such as high temperature fuel cells, or even renewable sources such as wind and solar. In the end, each project will need to define its own techno-economic boundaries and compare the best options according to custom targets. Energy system optimization can be a useful tool for researchers, ship operators, component integrators, and regulatory authorities to develop and analyze scenarios for sustainable system solutions.

6 DEFINITIONS, ACRONYMCS, ABBREVIATIONS

6.1 Acronyms

CAPEX	Capital expenditures / investment costs
CO_2	Carbon dioxide
H_2	Hydrogen
HFO	Heavy Fuel Oil
LH_2	Liquid Hydrogen
OPEX	Operational expenditures / operating costs
Re-MeOH	Renewable Methanol

6.2 Optimization variables

$C_{s,t}$	Charge of storage s at time t
CP_s	Storage capacity
$E_{c,c',t}$	Energy flow from component c into component c' at time step t
P_c^{max}	Maximum converter power

6.3 Parameters

η_c	Efficiency of converter c
$\eta_{s,roundtrip}$	Roundtrip efficiency of storage unit s
Δt	Time resolution
C_a	Annual costs
crf	Capital recovery factor
E_{CO_2}	Annual CO_2 emissions
$E_{d,t}$	Energy demand of component d at time step t
E_{eff}	Overall energy efficiency of system
$E_{s,t}$	Energy generation of source s at time step t
f_c	Fuel cost
I_c	Investment costs
O_c^{fix}	Fixed operating costs
O_c^{var}	Variable operating costs
P_g^{max}	Maximum power of grid g
P_s^{max}	Maximum charge/discharge power of storage s
R_c	Replacement costs
S_c	Salvage incomes
e_f	Fuel CO_2 emission intensity

7 ACKNOWLEDGEMENTS

The authors acknowledge the financial support of the "COMET - Competence Centres for Excellent Technologies" Programme of the Austrian Federal Ministry for Climate Action, Environment, Energy, Mobility, Innovation and Technology (BMK) and the Federal Ministry for Digital and Economic Affairs (BMDW) and the Provinces of Styria, Tyrol and Vienna for the COMET Centre (K1) LEC EvoLET. The COMET Programme is managed by the Austrian Research Promotion Agency (FFG).

8 REFERNCES & BIBLIOGRAPHY

[1] IEA , *World Energy Outlook 2022,* Paris : https://www.iea.org/reports/world-energy-outlook-2022, License: CC BY 4.0 (report); CC BY NC SA 4.0 (Annex A), 2022.

[2] International Maritime Organization, „Fourth Greenhouse Gas Study 2020," London, 2021.

[3] European Comission, „Reducing emissions from the shipping sector," European Comission, [Online]. Available: https://climate.ec.europa.eu/eu-action/transport-emissions/reducing-emissions-shipping-sector_en. [Access on 13.02.2023].

[4] ABS, „News Brief MEPC 79,“ American Bureau of Shipping, Spring, Texas, 2022.

[5] J. Kerse, N. D. Popovich und A. A. Phadke, „Rapid battery cost declines accelerate the prospects of all-electric interregional container shipping.,“ *Nature Energy,* Vol. 7.7, pp. 664-674, 2022.

[6] J. Hansson, S. Månsson, S. Brynolf und M. Grahn, „Alternative marine fuels: Prospects based on multi-criteria decision analysis involving Swedish stakeholders,“ *Biomass and Bioenergy,* Vol. 126, pp. 159-173, 2019.

[7] O. B. Inal, J.-F. Charpentier und C. Deniz, „Hybrid power and propulsion systems for ships: Current status and future challenges,“ *Renewable and Sustainable Energy Reviews,* Vol. 156, p. 111965, 2022.

[8] J. A. Ros, E. Skylogianni, V. Doedée, J. T. van den Akker, A. W. Vredeveldt, M. J. Linders, E. L. Goetheer und J. G. M. Monteiro, „Advancements in ship-based carbon capture technology on board of LNG-fuelled ships,“ *International Journal of Greenhouse Gas Control, Vol*. 114, p. 103575, 2022.

[9] B. Thaler, F. M. Kanchiralla, S. Posch, G. Pirker, A. Wimmer, S. Brynolf und N. Wermuth, „Optimal Design and Operation of Maritime Energy Systems Based on Renewable Methanol and Closed Carbon Cycles,“ *Energy Conversion and Management,* Vol. 269, p. 116064, 2022.

[10] B. Thaler, S. Posch, A. Wimmer und G. Pirker, „Hybrid Model Predictive Control of Renewable Microgrids and Seasonal Hydrogen Storage,“ *submitted ,* 2022.

[11] Burea Veritas, „White Paper Alternative Fuels Outlook for Shipping: An Overview of Alternative Fuels from a Well-To-Wake Perspective,“ Burea Veritas , 2022.

[12] A. D. Korberg, S. Brynolf, M. Grahn und I. R. Skov, „Techno-economic assessment of advanced fuels and propulsion systems in future fossil-free ships,“ *Renewable and Sustainable Energy Reviews,* Vol. 142, p. 110861, 2021.

[13] J. Kiviluoma und P. Meibom, „Influence of wind power, plug-in electric vehicles, and heat storages on power system investments,“ *Energy,* Vol. 35, pp. 1244-1255, 2010.

[14] F. M. Kanchiralla, S. Brynolf, E. Malmgren, J. Hansson und M. Grahn, „Life-Cycle Assessment and Costing of Fuels and Propulsion Systems in Future Fossil-Free Shipping,“ *Environmental Science & Technology,* Vol. 56, pp. 12517–12531, 2022.

[15] E. S. Hamborg und e. al., „Results from MEA testing at the CO2 Technology Centre Mongstad. Part II: Verification of baseline results.,“ *Energy Procedia,* Vol. 63, pp. 5994-6011, 2014.

[16] L. Vimmerstedt, „2021 Annual Technology Baseline (ATB) Cost and Performance Data for Electricity Generation Technologies,“ 2021.

[17] M. Taljegard, S. Brynolf, M. Grahn, K. Andersson und H. Johnson, „Cost-effective choices of marine fuels in a carbon-constrained world: results from a global energy model,“ *Environmental science & technology,* Vol. 48, pp. 12986-12993, 2014.

[18] Stena Bulk + Oil and Gas Climate Initiative, „Is carbon capture on ships feasible?,“ 2021.

[19] P. Balcombe, J. Brierley, C. Lewis, L. Skatvedt, J. Speirs, A. Hawkes und I. Staffell, „How to decarbonise international shipping: Options for fuels, technologies and policies,“ *Energy Conversion and Management,* Vol. 182, pp. 72-88, 2019.